

Research Journal of Pharmaceutical, Biological and Chemical Sciences

Possible Protective Effect Of Curcumin Encapsulated Nanoparticles Against Colon Carcinogenesis In Male Mice.

Farida E Elbassiouni*, Wafaa M El-Kholy, and El-Sayed M Elhabibi.

Zoology Department, Faculty of Science, Mansoura University, Egypt.

ABSTRACT

Colon cancer is the third most common cancer, there are previous studies demonstrated that nanocurcumin is safely used against different cancers and more effective than normal curcumin(CUR). Our study aim is studying the protection effect of CUR-encapsulated poly (lactic-coglycolic acid) (PLGA) nanoparticles (CUR@PLGA) against colon carcinogenesis induced by dimethyl hydrazine (DMH) in mice. Also performed to evaluate the potential effect of nanoparticles for enhancing CUR bioavailability. The mice were randomly divided into 6 groups. The control group. The DMH group. The CUR group, CUR@PLGA group, DMH and CUR group and DMH and CUR@PLGA group. The animals were sacrificed at the end of 6 weeks. The results showed using CUR@PLGA made a significant improvement in the level of oxidative stress markers and anti-oxidants. CUR@PLGA showed significant increase in tumor protein P53 level, caspase 3 and Bcl-2 associated X protein (BAX) also significant decrease on B cell lymphoma 2 (Bcl-2) level. The Aberrant crept foci (ACF) that represent the first stage on colon carcinogenesis is significantly reduced in number on CUR@PLGA group. Our study reveals that CUR@PLGA have a great effect on antioxidants, apoptotic proteins and ACF. So, it provides an insight towards the use of biological sources as promising anticancer agents.

Keywords: Nanocurcumin, colon cancer, ACF, P53, caspase 3, Bcl-2

<https://doi.org/10.33887/rjpbcs/2021.12.2.21>

**Corresponding author*

INTRODUCTION

Colorectal cancer (CRC), also called cancer of the large bowel. (CRC) is a global public health problem. CRC is the third most common cancer in men and the second most common cancer in women worldwide based on GLOBOCAN [1]. Many factors cause CRC such as modification of the intestinal microflora by certain dietary and lifestyle, spontaneous mutations or hereditary, abdominal radiation, Physical inactivity and obesity.

1, 2- dimethylhydrazine (DMH) used in chemically induced colon cancer in animal models. DMH oxidized to azoxymethane (AOM) and then hydroxylated to methylazoxymethanol (MAM) that can reach the intestine through bile, intestinal lumen directly and also via circulation, body temperature made it chemically unstable and decomposes to formaldehyde, water, nitrogen and (the alkylating agent) methyldiazonium ion, which generates a reactive carbonium ion capable of alkylating macromolecules (DNA, RNA, or protein) in the colon. [2].

Curcumin (CUR) the age-old medicine is a yellow-orange powder and water insoluble. CUR used as antiseptic, analgesic, anti-inflammatory, antioxidant, antimalarial, insect repellent, and other activities. CUR could mediate both pro-oxidant (chemicals that induce oxidative stress) and antioxidant (compounds that inhibit oxidation), that can produce free radicals[3]. CUR have anticancer effect on CRC one of them is the activation of the apoptosis pathways. CUR have anticancer effect on CRC one of them is the activation of the apoptosis pathways. ACF identified as the earliest recognizable lesions on the carcinogen-exposed rodent colons. ACF is bigger than the normal crypts in the field, also have epithelial cells that are thicker layer and stains darker and generally have oval openings. [4].

In spite of the large potential of CUR in cancer treatment, its absorption, distribution, metabolism, and excretion (ADME) studies showed extremely poor absorption of this molecule and rapid metabolism (low serum levels, limited tissue distribution, apparent rapid metabolism, and short half-life) that extremely decrease its bioavailability [5].

Nanotechnology is the branch of science that usually work with the size range from a few nanometers (nm) to several hundred nm, depending on their intended use. It offers numerous benefits to overcome the limitations of conventional formulations of the drugs. Polymer nanoparticles have small size and excellent biocompatibility so it is widely used in nanotechnology. Synthetic polymers include PLGA that considered an efficient choice for the formulation of a variety of nondrug. Researchers approved the effectiveness of various types of PLGA nanoparticles for curcumin encapsulation [6].

MATERIALS AND METHODS

Chemicals

1, 2- dimethylhydrazine (DMH) (purity 99.9%) was obtained from Sigma-Aldrich Co. (Saint Louis, MO, USA). methylene blue, PLGA, Curcumin, PLGA (50:50 lactide–glycolide MW=24000:38000) was purchased from sigma Aldrich (Germany). Poly (vinyl alcohol) (PVA) (M.W. 30,000–70,000) Advant, India, curcumin (ACS reagent grade) were purchased from Loba-Chemie. Di-chloromethane purchased from Macron Fine Chemicals™.

(CUR@PLGA) preparation

Curcumin-encapsulated nanoparticles were prepared according to the solid-in-oil-in-water (s/o/w) emulsion technique [7]. PLGA (45 mg) was dissolved in dichloromethane for 6 h to obtain a uniform PLGA solution. Normal curcumin was added to the PLGA solution and sonicated at 55 W for 1 min to produce the solid-in-oil primary emulsion. This emulsion was added to 20 ml of polyvinyl alcohol solution (1% w/v) and again sonicated at 55 W for 2 min to get the final solid-in-oil-in-water emulsion. The resulted nano-sized particles were stirred in the emulsion for 3 h for solvent evaporation. The final emulsion was centrifuged at 15,000 g for 15 min to remove the residual solvent. The nanoparticles obtained were washed thrice with deionized distilled water, and finally resuspended in deionized water and dried on a lyophilizer. The nanoparticles were stored at 4 °C till further use.

Characterization of CUR@PLGA nanoparticles

CUR@PLGA nanoparticles were characterized using various analytical techniques, Transmission Electron Microscopy (TEM), the Fourier Transform Infrared (FT-IR) spectroscopy, zeta potential, and encapsulation efficiency (EE).

Particle size and morphology by transmission electron microscopy (TEM)

The size and morphology of the nanoparticles were determined using a TEM (JEM-2100 HR) at National Research Center, Egypt. A copper coated-carbon grid was placed in the CUR-NP solution (1 mg/ml) for 15 minutes before drying on a filter paper. The grid was then loaded into the TEM and the size and morphology were determined. The TEM images revealed that the morphology of PLGA and CUR@ PLGA are spherical shape with mean diameter 15 ± 2 nm as shown in Fig. I (a, b) PLGA and CUR @ PLGA respectively.

Fourier-transform infrared spectroscopy (FTIR)

The infrared spectra were recorded on a Fourier transform infrared spectrometer Vertex 70 RAM II (Germany) at National Research Center in order to obtain information about chemical groups present around CUR@PLGA for their stabilization and understand the transformation of functional group due to capsulation process. FT-IR spectra of CUR, PLGA and CUR@PLGA are shown at Fig. II (FTIR a,b and c) respectively.

At Fig. II (FTIR a); Infrared of CUR show stretching vibration at 3497 cm^{-1} due to O-H groups. CUR revealed different peaks of different function groups where in the area FTIR (a i); bands at 1627 cm^{-1} assigned to stretching vibrations of alkenes (C=C), peaks at 1600 cm^{-1} assigned to aromatic alkenes C=C, 1512 cm^{-1} assigned to vibrated (C=O), 1465 cm^{-1} assigned to stretching (CH_3), 1425 cm^{-1} assigned to (OH) bending vibration, 1377 cm^{-1} (CH) bending 2 (CH_3) groups and the peak at 1316 cm^{-1} (OH) bending. Furthermore, significant intense band at 1277 cm^{-1} attributed to the bending vibration of the (C – O) phenolic band. These assignments are in good agreement with the assignments of [8].

While at region of FTIR (a ii) peaks at, 1230 cm^{-1} assigned to C-O stretching vibrations and the range from $1205 - 1026 \text{ cm}^{-1}$ assigned to aromatic C-H. These assignments are in good agreement with the assignments of [9].

Also the region of FTIR (a iii) peaks at 986 and 959 cm^{-1} assigned to C=C bending, 887 , 856 , 808 , 785 , 747 and 717 cm^{-1} assigned to (C-H) bending. These assignments are in good agreement with the assignments of [9]. Meanwhile the region of FTIR (a iv) peaks at 623 , 600 , 575 , 562 , 542 , 466 and 450 cm^{-1} assigned to aromatic C-C-C bending.

Fig. II (FTIR b) indicates identical PLGA peaks at 850 , 1643 and 3300 cm^{-1} referring to C-H bending, C=O stretching and O-H stretching respectively.

Finally, after encapsulation of CUR@PLGA Fig. II (FTIR c) showed complete hidden of CUR peaks except the 1043 cm^{-1} peak which corresponding to O-CH₃ bond involved with the aforementioned PLGA peaks.

Encapsulation efficiency and loading capacity:

We conducted differential absorption method in order to determine the encapsulation efficiency (EE). We measured the absorption of supernatant which represents the amount of NP's left after centrifugal precipitation of drug added (W_t) and extracted (W_f) of the capsulated-nanoparticles. The encapsulation efficiency was measured by using a UV-Vis spectrophotometer (Cary series UV-Vis-NIR, Australia). The CUR was detected at 420 nm (excitation).

The EE parameter was calculated as followed:

$$EE\% = \frac{W_t - W_f}{W_t} * 100$$

Loading capacity (LC %) can be calculated as shown in Fig. III by the amount of total encapsulated drug divided by the total nanoparticle weight. Initial Concentration = 3 mg/ml .

Animals and Housing

Sixty male albino mice with body weight (15 – 20) gm used in our experiment, the mice obtained from Egyptian Institute for Serological and Vaccine production, Helwan, Egypt. Mice placed in a clean polypropylene cages with a wire mesh top with hygienic bed of sawdust (regularly changed every 2 days) and were maintained in a well-ventilated room ($25 \pm 1^\circ\text{C}$ with $55 \pm 5\%$ humidity) and a 12 h light/dark cycle. The mice were acclimatized with standard laboratory diet and water ad libitum for one week before commencement of the experiment. All animal procedures were conducted in accordance with the standard guidelines for care and use of laboratory animals. The protocol was approved by Mansoura University, Faculty of science, and department of zoology ethics committee on the use of the experimental animals for researches.

Experimental Design

The mice received a 1-week period of acclimation and were randomly divided into four groups of 6 animals. The 1st served as normal control group. DMH- subcutaneously (S.C.) injected mice group (**DMH group**) (10 mg/kg body weight(bw) dissolved in 0.2 ml saline once a week for three consecutive weeks (0,1st and 2nd weeks(wk.))[10], **CUR group** the mice were oral administered curcumin [10 mg/kg bw six times a wk for six consecutive wks.][11]. **CUR @ PLGA group** the mice were oral administered curcumin encapsulated PLGA [10 mg/kg bw six times a wk. for six consecutive wks.] [12]. **DMH+ CUR group** mice were injected with DMH at the same dose in DMH group and administered curcumin in the same dose in CUR group. **DMH+ CUR @ PLGA group** mice were injected with DMH at the same dose in DMH group and administered curcumin encapsulated PLGA in the same dose in CUR @ PLGA group. **All mice were fasted 12 hr and sacrificed under light ether anesthesia.** Blood samples were individually collected from the retro orbital bleeding of each mice in non-heparinized glass tubes. Sera were separated by centrifugation at 3000 rpm for 15 minutes. The collected sera were stored at -20°C until analysis. Animals were then dissected and colon from each mice removed, rinsed in ice-cold physiological saline and dried with filter paper. Specimens of colon were weighted and homogenized for biochemical analysis, while others were fixed in 10% neutral formalin for ACF analysis.

Aberrant Crypt Analysis

Colon whole mounts were removed from 10% phosphate buffered formalin and stained with 0.02% methylene blue in distilled water for 2-5 minute [13]. Samples were examined for the presence of ACF by a compound microscope at x10 magnifications.[14] The number of aberrant crypts in each focus was counted and divided by the total numbers of aberrant crypts to evaluate the crypt multiplicity. ACF that showed variations in its multiplicity, such as foci containing 1 crypt (1AC), foci with 2 or 3 crypts (2ACs and 3ACs), or larger foci with- or more than 4 crypts (≥ 4 ACs), were counted and separated in categories. Capture images were shot, and then the samples were stored again in buffered formalin.

Preparation of colon tissue suspension for flowcytometry

Fresh tissue specimens from the colon were used in isotonic saline 0.9% and prepared as follow:

1. The material was washed with isotone tris EDTA buffer, [3.029 gm of 0.1 M tris (hydroxymethylaminomethane, 1.022 gm of 0.07 M sodium chloride (ADWIC) and 0.47 gm of 0.005 M EDTA].
2. They were dissolved in 250 ml of distilled water and then adjust the pH at 7.5 by using 1N HCl.
3. Then, the cell suspension was centrifuged at 1800 rpm for 10 mins., where upon the supernatant was aspirated. If they were macroscopically contaminated with blood, it was then subjected to haemolysis with filtered tap water for 10 mins.
4. After centrifugation and aspiration of the supernatant the cell is fixed in ice-cold 96-100% ethanol (BDH) in approximately 1 ml for each sample.

The fixed cells can be stored indefinitely in a refrigerator and can also be mailed without running the sample [15].

Determination of the oxidative stress and antioxidant levels on colon tissue

All markers we measured were assayed by using clear supernatants of colon tissue homogenates. These assays including: i) peroxidation reactions Products: Lipid peroxidation (LPO) was measured by by assaying the end product of

peroxidation reaction malondialdehyde (MDA) and the result was expressed as (nmol/g wet tissue) [16]. ii) measuring of nitric oxide (NO) by griess method and the result was expressed as ($\mu\text{mol/g}$ wet tissue) [17]. iii) protein carbonyl (PC) determination is measured according to [18] and expressed as (nmol/g) total protein. iiiii)Antioxidant enzymes: Total Antioxidant Capacity (TAC) was determined and expressed as mM/g [19]. While Catalase Activity (CAT) was assayed and expressed as Unit per gram of tissue (U/g) [20]. Also superoxide dismutase (SOD) activity was estimated [21] and expressed as (U/g). Finally, Glutathione (GSH) content was determined with dithionitrobenzoic acid using the method described by [22]. and was expressed in(mmol\g). Glutathione-S-transferase (GST) was determined at 340 nm using 1-chloro-2,4-dinitrobenzene as a substrate according to the method described by [23] and also expressed as (U /g tissue). All analysis assayed on semi Auto Biochemistry Analyzer (Robonik).

Determination of (Bcl-2) , Apoptosis regulator BAX , Caspase 3 and the P53 in colon tissue

1. 100 μl of cell suspension (1×10^6) cell/ml was prepared by isolation of mononuclear cells from any ascites or body fluid or processing of tissue with tris edeta buffer (TEB).
2. The cells were washed with phosphate buffer solution PBS/BSA (Bovine serum albumin) with 2 ml and then centrifuged at 2000 rpm for 5 min.
3. The supernatant was discarded and suspended the pellet in 100 μl of PBS.
4. 7 μl of any marker (Bcl-2, BAX, Caspase 3 or P53) was mixed well then incubated the tube for 30 min at room temperature in dark.
5. Cells were washed twice with 2 ml PBS/BSA; and were centrifuged at 2000 rpm for 5 min and the supernatant was discarded.
6. Finally, cells were suspended in 200 μl of 4% par formaldehyde in PBS and then fixed until acquired by BD Accuri C6 flowcytometer [24].

Identification of Aberrant crypt foci (ACF)

Colon whole mounts were removed from 10% phosphate buffered formalin and stained with 0.02% methylene blue in distilled water for 2-5 minute [13]. Samples were examined for the presence of ACF by a compound microscope at $\times 10$ magnifications [14]. The number of aberrant crypts in each focus was counted and divided by the total numbers of aberrant crypts to evaluate the crypt multiplicity. ACF that showed variations in its multiplicity, such as foci containing 1 crypt (1AC), foci with 2 or 3 crypts (2ACs and 3ACs), or larger foci with- or more than 4 crypts (≥ 4 ACs), were counted and separated in categories. Capture images were shot, and then the samples were stored again in buffered formalin.

Statistical analysis

The results expressed as mean \pm standard error (SE). All data were analyzed by one-way analysis of variance (ANOVA) followed by least significant difference (LSD) test. The analysis was conducted using SPSS statistical package, version 19.00 software. $P \leq 0.05$ was considered statistically significant [25].

RESULTS

Markers of Oxidative Stress

As shown in **Table (1)** and **Fig. 1 (a-c)**, administration of CUR, PLGA or CUR@PLGA did not show any significant change in MDA, PC and NO levels when compared with control group. DMH group showed significant increases in comparison with normal control group. DMH+CUR and DMH+CUR@PLGA groups significantly reduced the oxidative stress markers levels as compared to DMH group but MDA and NO levels still significantly higher than normal control. DMH+CUR@PLGA group showed complete recovery on PC level. On the other hand DMH+PLGA group showed non-significant effect on the tested parameters level when compared to DMH group. The greatest improvement appeared on DMH+CUR@PLGA group.

Markers of anti-oxidants

As shown in **Table (2)** and **Fig.2 (a-e)**, CUR, PLGA and CUR@PLGA groups did not show any significant change in SOD, CAT, GSH, GST and TAC levels when compared with normal control group. DMH group showed significant decrease in antioxidants activities levels as compared to normal control group. DMH+CUR group showed non-significant increase in GST and TAC and significant increase in SOD, CAT and GSH levels when compared with DMH group but still significantly less than

normal control group. DMH+CUR@PLGA significantly increase the SOD, CAT, GSH, GST and TAC levels as compared to DMH group and also showed complete recovery except on SOD activity it still have significant difference with control group.

On the other hand DMH+ PLGA group showed non-significant effect on the tested parameters level when compared with DMH group.

Apoptotic proteins

As shown in Table (3) and Fig.3 (a-e), CUR and PLGA groups didn't show any significant change when compare with normal control group on the other hand CUR@PLGA group showed non-significant increase on P53 level and significant increase on Caspase 3 and BAX also significant decrease on Bcl-2 level as compared to DMH group. Administration of DMH resulted in significant decrease in P53, Caspase 3 and BAX and significant increase on Bcl-2 levels as compared to normal control group.

DMH+CUR and DMH+CUR@PLGA groups showed significant increase in the P53, Caspase 3 and BAX levels and significant reduce in Bcl-2 level as compared to DMH group. Meanwhile DMH+PLGA group showed non-significant effect on the tested parameters level when compared with DMH group.

Effect of curcumin, PLGA and their nano loading on DMH-induced apperant crep foci(ACF) Formation

Table4 and Fig.4 (a, b and c) show the total numbers of ACF as well as the numbers of different crypt criteria. It was found that the mice in DMH+CUR group had significant lower total numbers of ACF ($P<0.05$) as compared with the DMH group. DMH+CUR@ PLGA group showed the lowest significant number of total ACF when compared with DMH group. Interestingly, all treatments have significantly reduced the ACF (≥ 4 ACs) numbers, which are expected to develop into tumors. Fig.4b showed the shapes of ACF and its multiplicities of crypt while colon stained with methylene blue stain.

Table 1: Data for average of oxidative stress markers NO, MDA and PC in different groups.

| | control | CUR | PLGA | CUR@PLGA | DMH | DMH+CUR | DMH+PLGA | DMH+CUR@PLGA |
|---------------------|-----------------|-----------------|----------------|-----------------|-----------------------------|--------------------------------|-----------------------------|--------------------------------|
| MDA (nmol\g) | 1454.8 ±12.6 | 1453 ±11.8 | 1453.6 ±9.9 | 1451.4 ±10.1 | 2385.5 ^a ±8.4 | 1974.5 ^{a,b} ±11.0 | 2379.5 ^a ±6.5 | 1680.2 ^{a,b} ±7.1 |
| PC (ng\ml) | 0.59 ±0.071 | 0.57 ±0.07 | 0.58 ±0.08 | 0.53 ±0.09 | 4.92 ^a ±0.18 | 2.60 ^{a,b} ±0.10 | 4.87 ^a ±0.28 | 1.04 ^b ±0.18 |
| NO (µmol/g) | 130.75 ±2.36 | 129.66 ±2.21 | 131.58 ±2.7 | 129.08 ±2.7 | 282.2 ^a ±2.35 | 223.25 ^{a,b} ±1.71 | 280.6 ^a ±1.85 | 160.32 ^{a,b} ±2.19 |

Values are expressed as mean ± SE for 6 animals in each group.

CUR= curcumin, **PLGA**= (Poly Lactic -co- Glycolic Acid), **CUR@PLGA**= Curcumin encapsulated PLGA, **DMH**= (dimethyle hydrazine).

Values have different superscripts represent statically significant differences ($p<0.05$).

a, b Compared different groups with control and DMH respectively.

Table 2: Data for average of anti-oxidants SOD, CAT, GSH, GST and TAC in different groups.

| | control | CUR | PLGA | CUR@PLGA | DMH | DMH+CUR | DMH+PLGA | DMH+CUR@PLGA |
|----------------------|-----------------|-----------------|-----------------|-----------------|-----------------------------|--------------------------------|----------------------------|--------------------------------|
| SOD (U/g) | 292.25 ±1.99 | 293.70 ±2.60 | 293.66 ±4.61 | 297.70 ±4.86 | 102 ^a ±2.82 | 137 ^{a,b} ±3.72 | 105 ^a ±3.29 | 266.44 ^{a,b} ±1.93 |
| CAT (U/g) | 190.75 ±3.8 | 194.08 ±3.95 | 193.25 ±4.21 | 195.66 ±3.5 | 71.58 ^a ±3.96 | 103.25 ^{a,b} ±2.98 | 72.83 ^a ±3.5 | 187.58 ^b ±3.65 |
| GSH (mmol /g) | 67.75 ±3.09 | 68.25 ±3.63 | 67.83 ±4.07 | 68.66 ±5.17 | 31.58 ^a ±2.98 | 47.5 ^{a,b} ±3.36 | 33.33 ^a ±3.0 | 63.66 ^b ±2.97 |
| GST (ng/ml) | 6.94 ±0.44 | 7.34 ±0.42 | 7.25 ±0.45 | 7.66 ±0.69 | 3.45 ^a ±0.23 | 4.50 ^a ±0.35 | 3.54 ^a ±0.32 | 5.82 ^b ±0.34 |
| TAC (mM / g) | 1.59 ±0.06 | 1.60 ±0.08 | 1.6 ±0.07 | 1.60 ±0.06 | 1.09 ^a ±0.08 | 1.22 ^a ±0.09 | 1.09 ^a ±0.07 | 1.56 ^b ±0.07 |

Values are expressed as mean ± SE for 6 animals in each group.

CUR= curcumin, **PLGA**= (Poly Lactic -co- Glycolic Acid), **CUR@PLGA**= Curcumin encapsulated PLGA, **DMH**= (dimethyle hydrazine).

Values have different superscripts represent statically significant differences (p<0.05).

a, b Compared different groups with control and DMH respectively.

Table 3: Data for average of apoptotic proteins P53, Caspase 3, BAX and Bcl-2 in different groups.

| | control | CUR | PLGA | CUR@PLGA | DMH | DMH+CUR | DMH+PLGA | DMH+CUR@PLGA |
|---------------------------------|----------------|----------------|----------------|-----------------------------|-----------------------------|-------------------------------|-----------------------------|-------------------------------|
| P53 (% count/ml) | 61.08 ±1.14 | 63.17 ±1.11 | 61.33 ±1.10 | 63.92 ±1.00 | 24.47 ^a ±0.62 | 40.25 ^{a,b} ±0.68 | 26.17 ^a ±0.87 | 50.50 ^{a,b} ±0.99 |
| Caspase 3 (%of count/ml) | 82.36 ±0.34 | 84.13 ±0.23 | 83.17 ±0.24 | 84.85 ^a ±0.44 | 35.45 ^a ±0.24 | 60.09 ^{a,b} ±0.42 | 35.69 ±0.37 | 72.22 ^{a,b} ±0.31 |
| Bax (%of count/ml) | 76.26 ±0.56 | 77.26 ±0.70 | 76.55 ±0.61 | 79.05 ^a ±0.70 | 42.09 ^a ±0.68 | 53.76 ^{a,b} ±0.77 | 43.59 ^a ±0.55 | 70.66 ^{a,b} ±0.59 |
| Bcl-2 (%of count/ml) | 22.27 ±0.41 | 21.22 ±0.45 | 21.85 ±0.39 | 20.65 ^a ±0.35 | 57.85 ^a ±0.39 | 38.57 ^{a,b} ±0.34 | 57.28 ^a ±0.35 | 14.80 ^{a,b} ±0.37 |

Values are expressed as mean ± SE for 6 animals in each group.

CUR= curcumin, **PLGA**= (Poly Lactic -co- Glycolic Acid), **CUR@PLGA**= Curcumin encapsulated PLGA, **DMH**= (dimethyle hydrazine).

Values have different superscripts represent statically significant differences (p<0.05).

a, b Compared different groups with control and DMH respectively.

Table 4: Effect of PLGA, Curcumin or Their Nano loading on DMH-Induced ACF Formation in mice

| | control | CUR | PLGA | CUR@PLGA | DMH | DMH+CUR | DMH+PLGA | DMH+CUR@PLGA |
|--------------------|-------------|-------------|-------------|-------------|---------------------------|-----------------------------|---------------------------|-----------------------------|
| Total (ACF) | 0.0 ±0.0 | 0.0 ±0.0 | 0.0 ±0.0 | 0.0 ±0.0 | 86.3 ^a ±2.2 | 75.3 ^{a,b} ±2.2 | 82.3 ^a ±3.1 | 48.7 ^{a,b} ±3.6 |

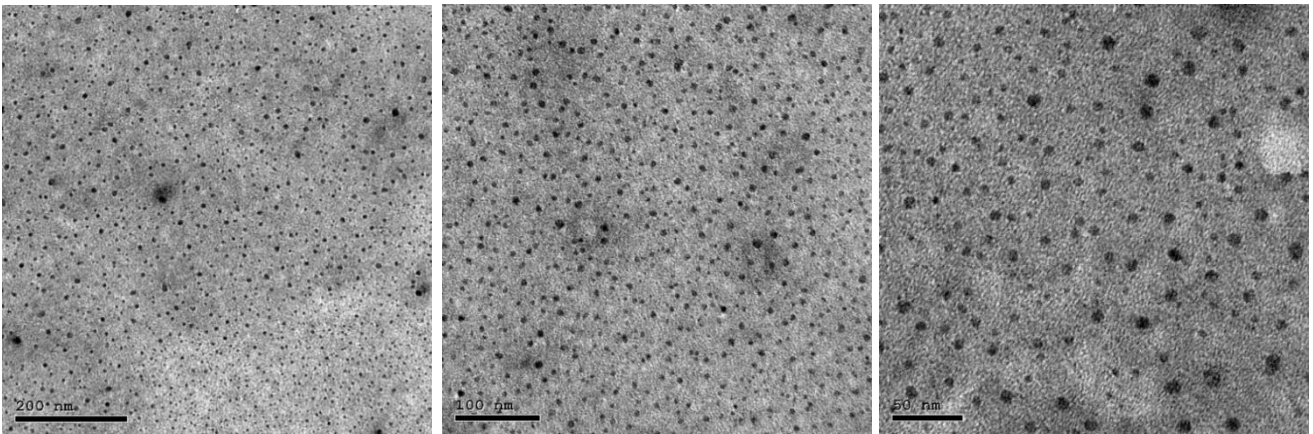
Values are expressed as mean ± SE for 6 animals in each group.

CUR= curcumin, **PLGA**= (Poly Lactic -co- Glycolic Acid), **CUR@PLGA**= Curcumin encapsulated PLGA, **DMH**= (dimethyle hydrazine).

Values have different superscripts represent statically significant differences (p<0.05).

a, b Compared different groups with control and DMH respectively.

(a)



(b)

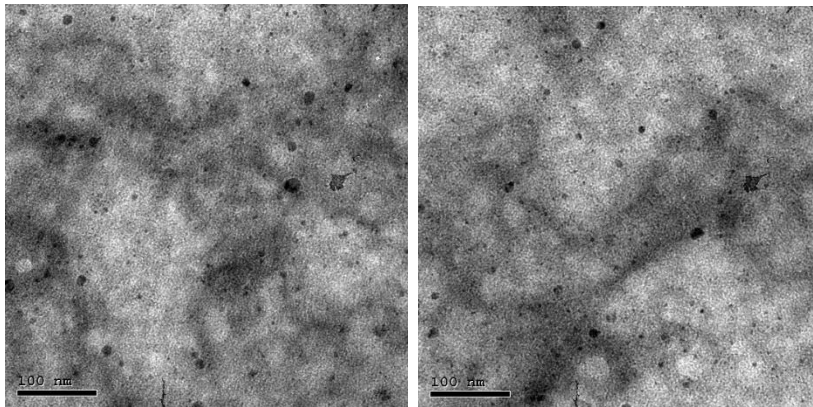


Fig. I (a & b): TEM micrograph of spherical shape synthesized PLGA and CUR@PLGA nanoparticles with mean diameter of particle $\approx 15 \pm 2$ nm.

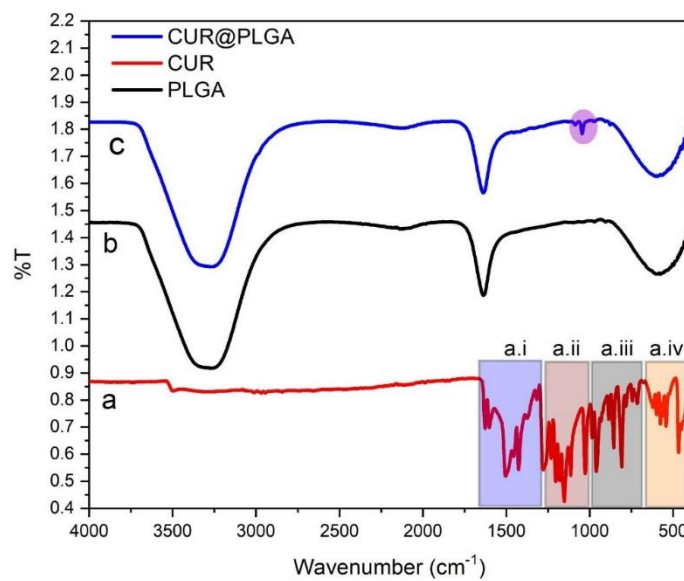
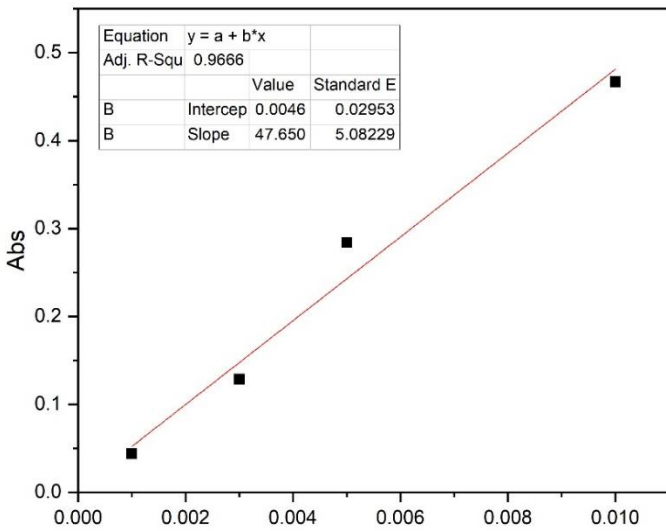


Fig. II: FTIR spectrum of (a) CUR, (b) PLGA, and (c) CUR@PLGA

Fig. III: Determination of the encapsulation efficiency



Abs = 0.00461 + 47.65028 X Conc.

Supernatant Abs = 2.87

Free Concentration = 0.0864 mg/ml

$$E.E = \frac{\text{Initial Con.} - \text{Free Conc.}}{\text{Initial Con.}} \times 100 = 97.12 \%$$

Loading capacity = 9.712 %

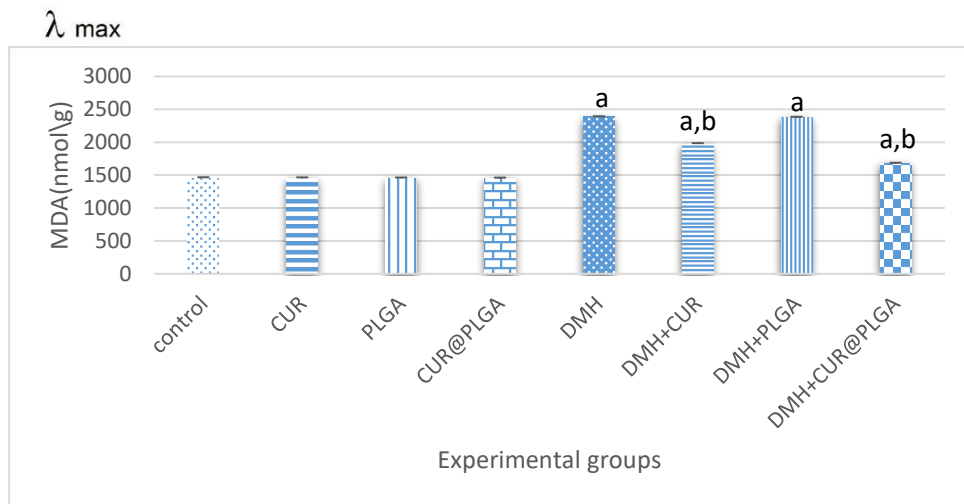


Fig. 1(a): The effect of curcumin, PLGA or Curcumin encapsulated PLGA on oxidative stress (MDA) of experimental groups P<0.05

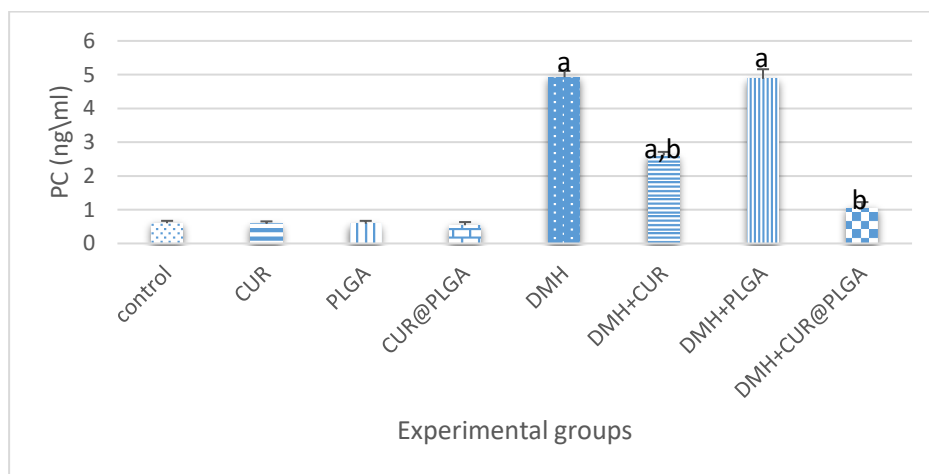


Fig. 1(b): The effect of curcumin, PLGA or Curcumin encapsulated PLGA on oxidative stress (PC) of experimental groups P<0.05

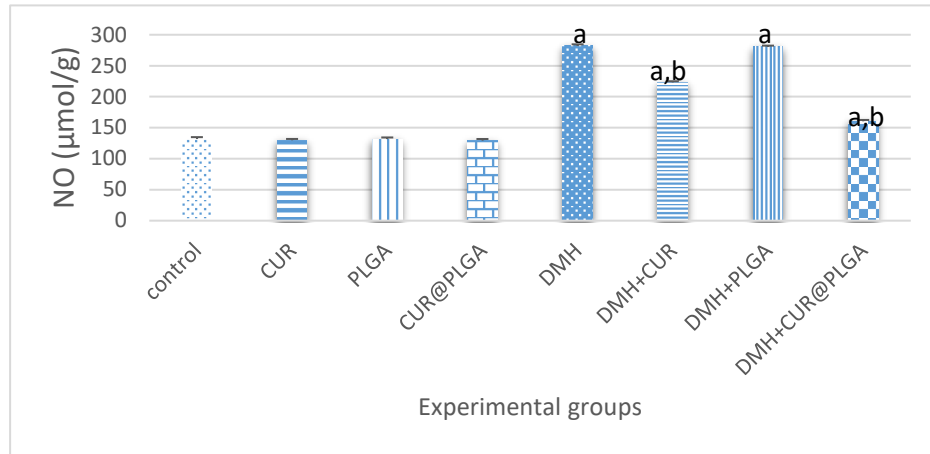


Fig. 1(c): The effect of curcumin, PLGA or Curcumin encapsulated PLGA on oxidative stress (NO) of experimental groups P<0.05

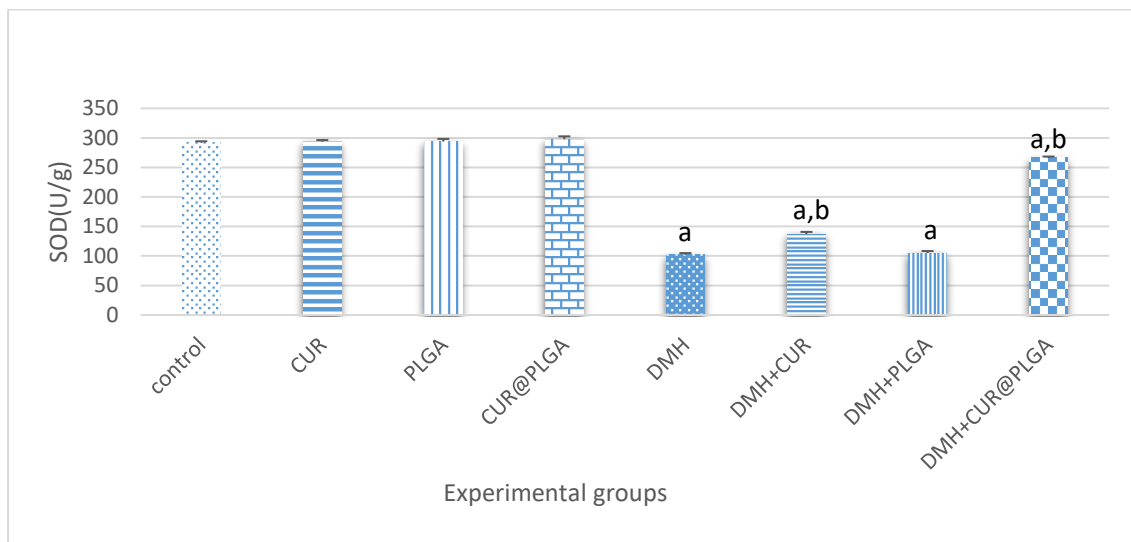


Fig. 2(a): The effect of curcumin, PLGA or Curcumin encapsulated PLGA on antioxidant (SOD) of experimental groups P<0.05

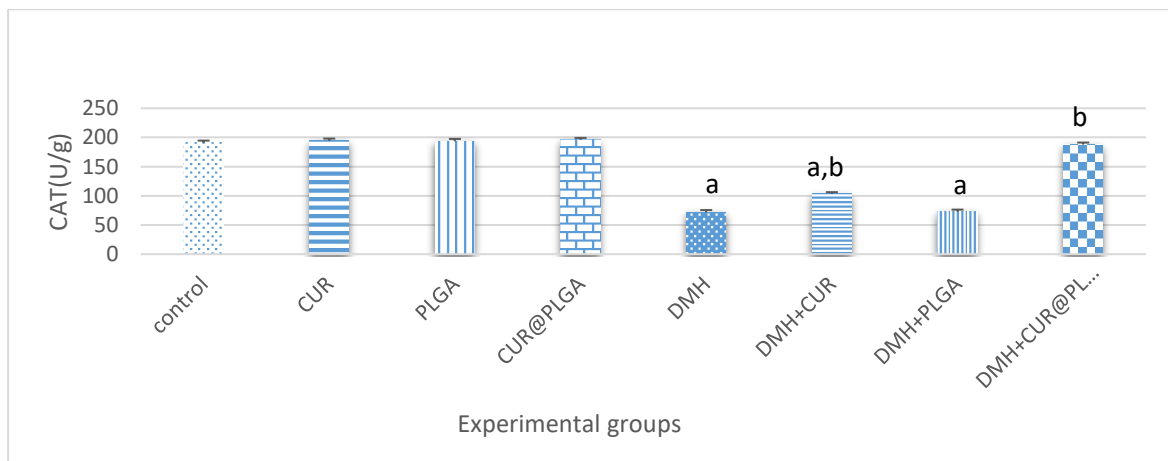


Fig. 2(b): The effect of curcumin, PLGA or Curcumin encapsulated PLGA on antioxidant (CAT) of experimental groups

P<0.05

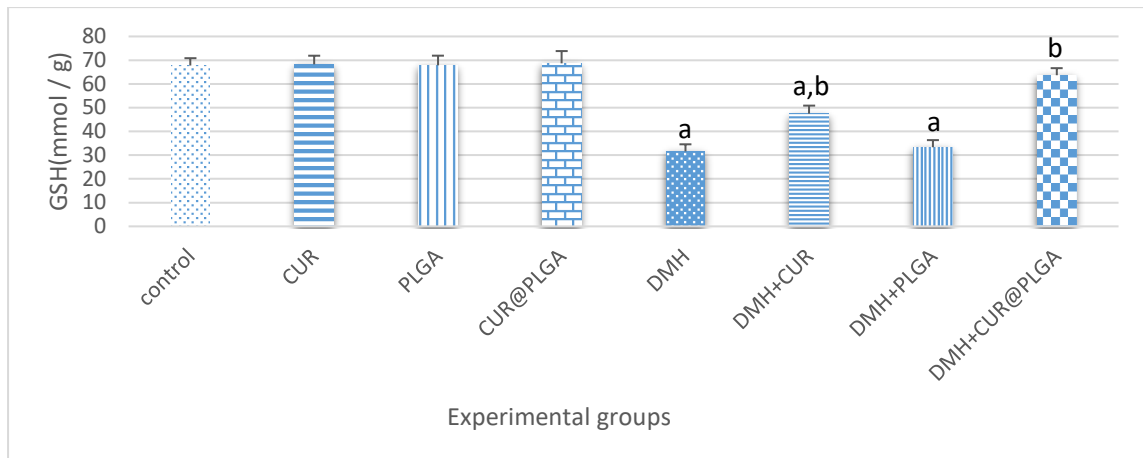


Fig. 2(c): The effect of curcumin, PLGA or Curcumin encapsulated PLGA on antioxidant (GST) of experimental groups

P<0.05

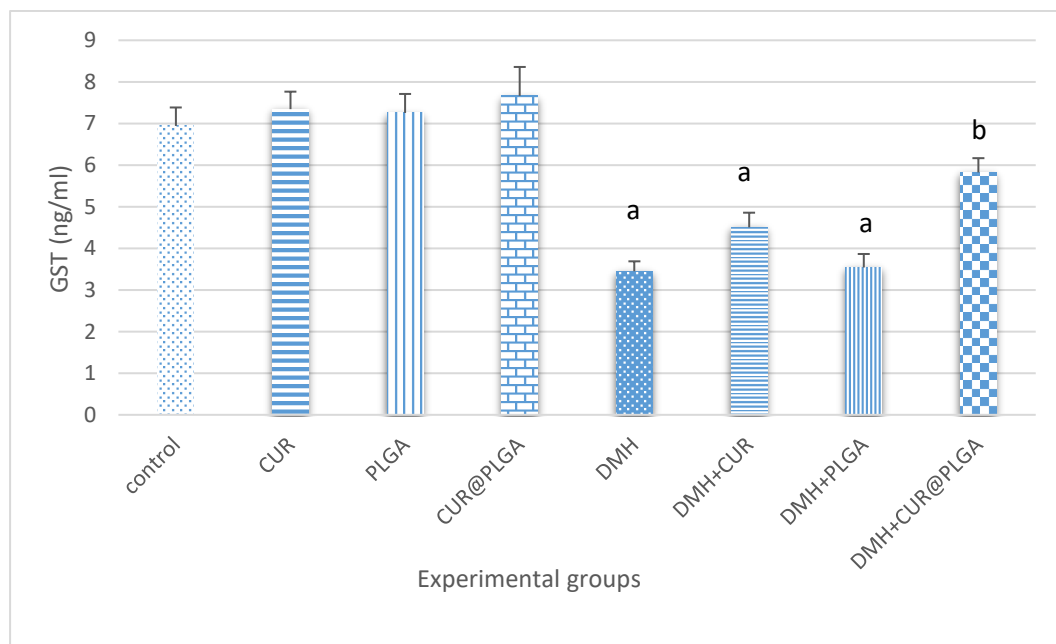


Fig. 2(d): The effect of curcumin, PLGA or Curcumin encapsulated PLGA on antioxidant (GST) of experimental groups

P<0.05

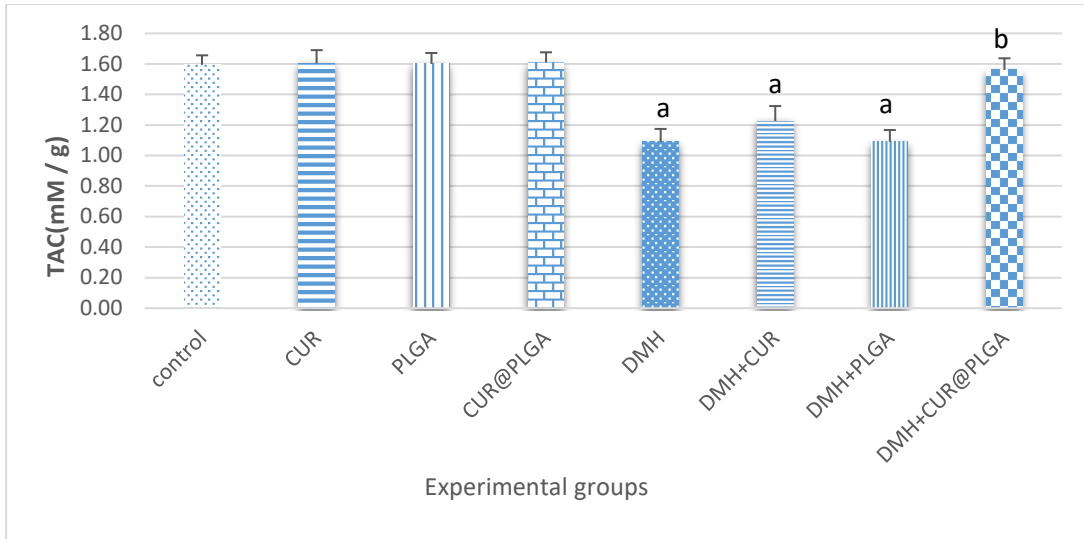


Fig. 2(e): The effect of curcumin, PLGA or Curcumin encapsulated PLGA on antioxidant (TAC) of experimental groups

P<0.05

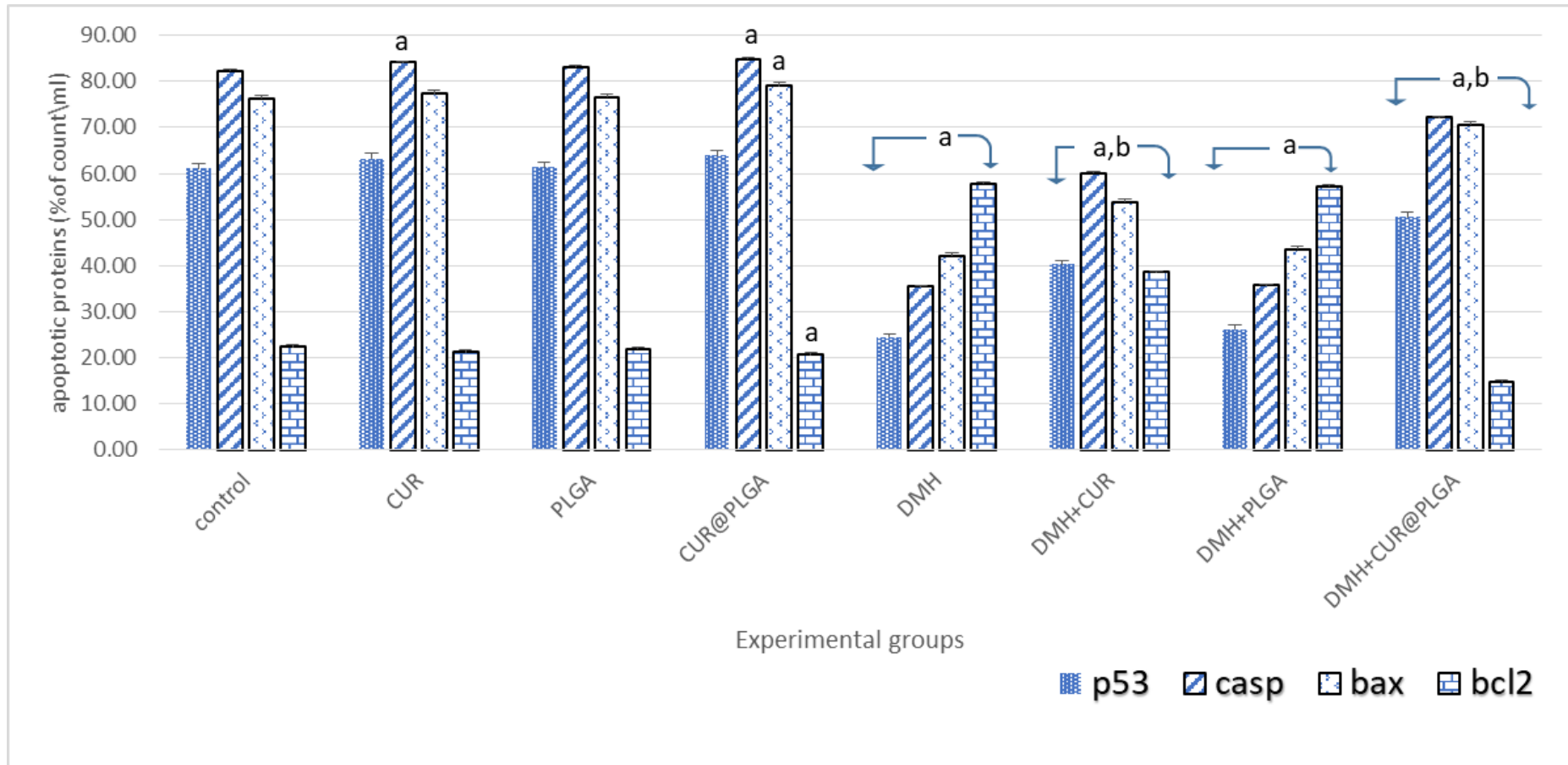


Fig. 3(a): percentages of apoptotic proteins (P53, Caspase 3 ,Bax and Bcl-2)

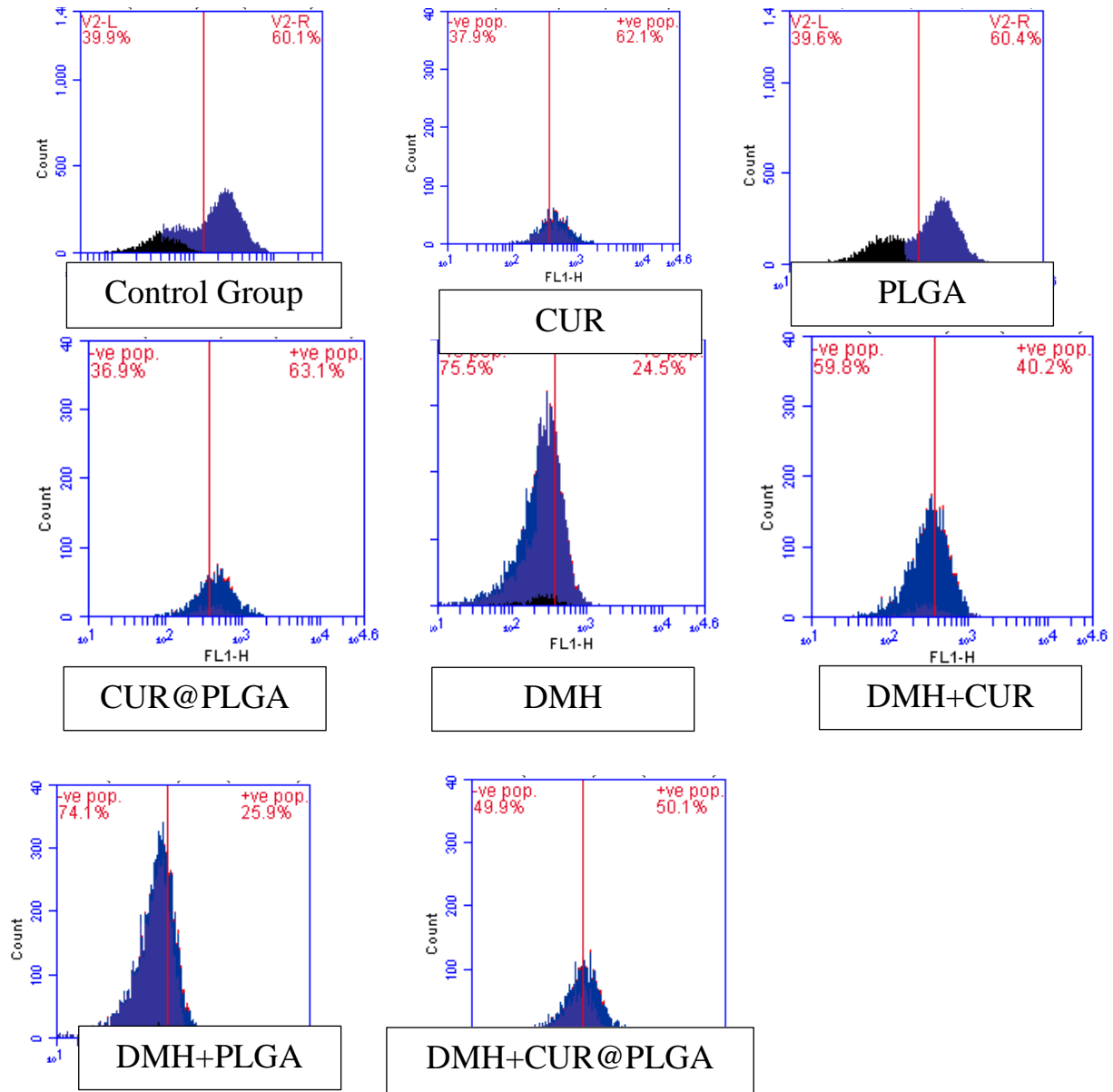
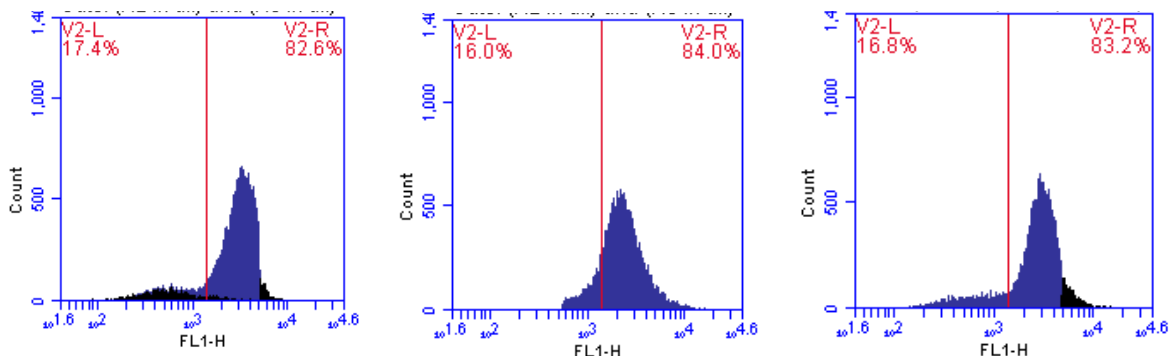


Fig. 3 (b): P53 %cell in control and different treated groups.

FLI-H: detector of P53 of Fluroseisothiocyanate (FITC)flourchrome.

Count: % of count cells labeled with anti P53



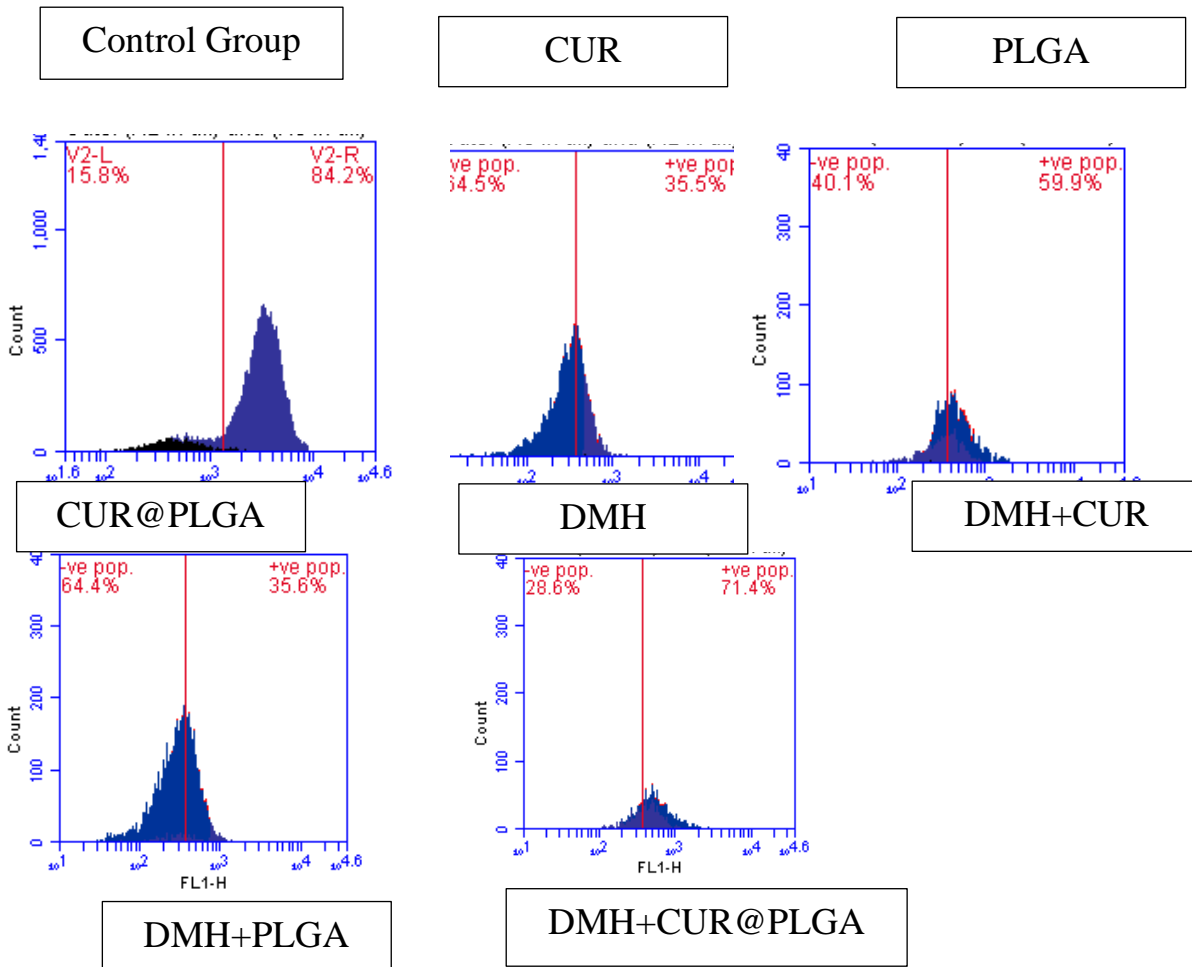
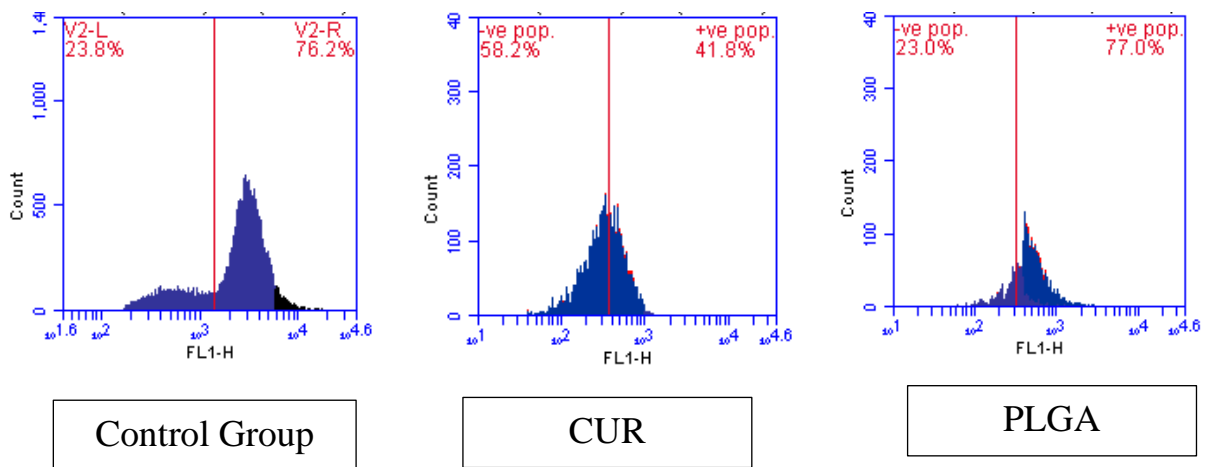


Fig. 3 (c): Caspase 3 %cell in control and different treated groups.

FLI-H: detector of P53 of Fluorescein isothiocyanate (FITC) fluorochrome.

Count: % of count cells labeled with anti Caspase 3.



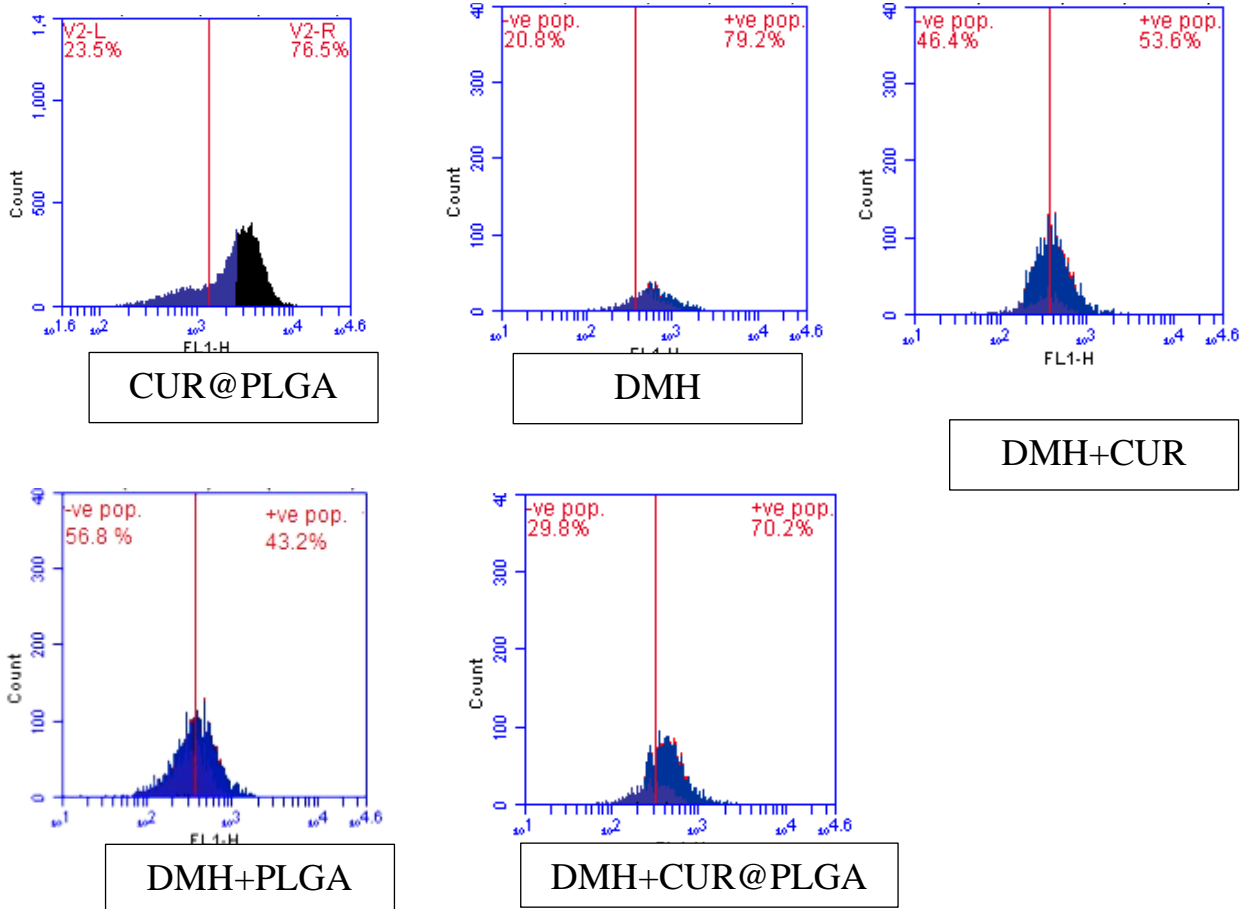
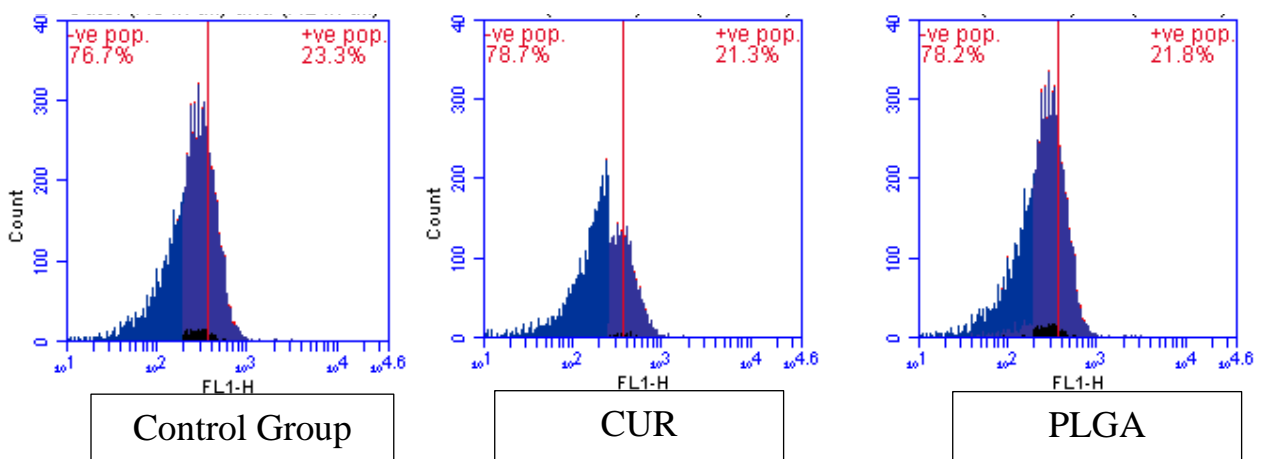


Fig. 3(d): Box %cell in control and different treated groups.

FLI-H: detector of P53 of Fluroseisothiocyanate (FITC)flourchrome.

Count: % of count cells labeled with anti Bax



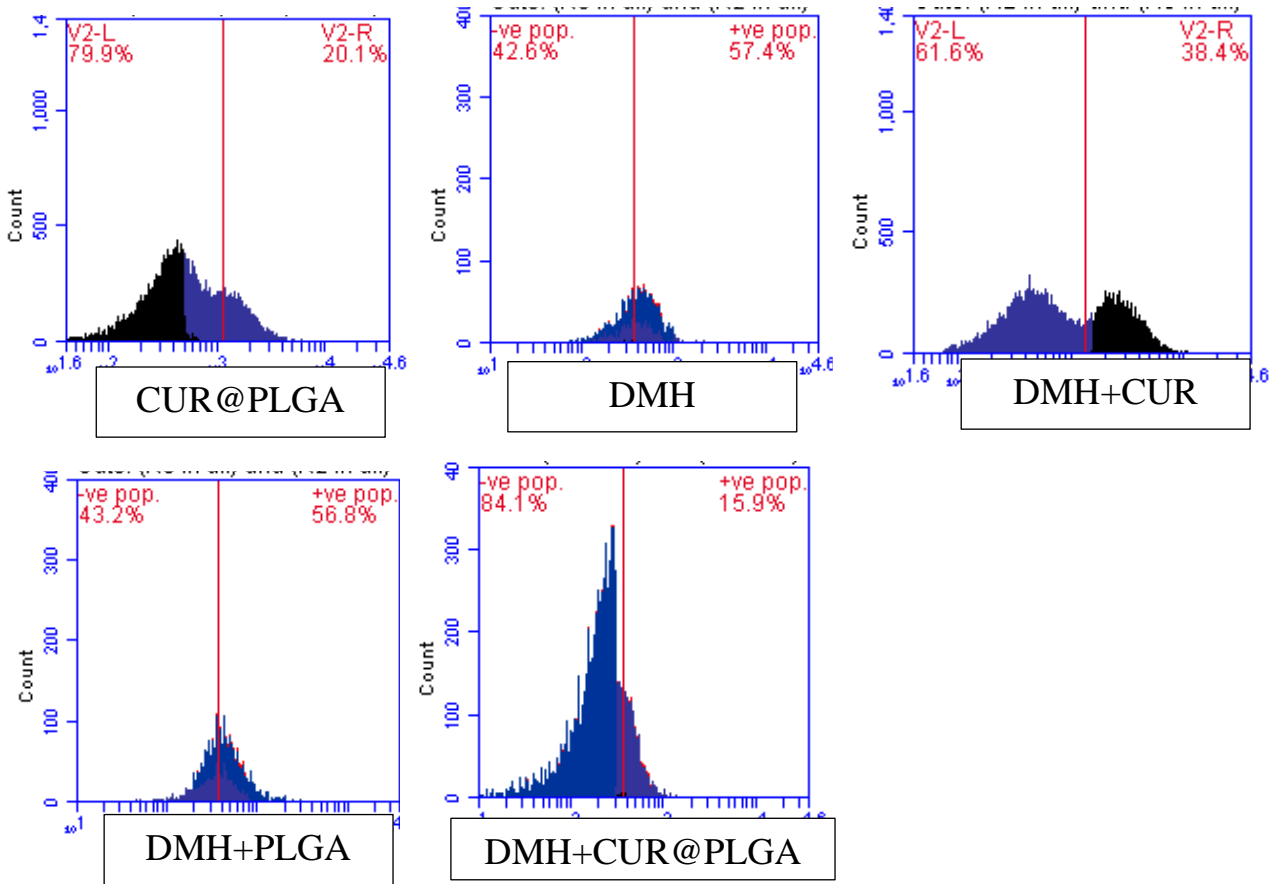


Fig. 3 (e): Bcl-2 %cell in control and different treated groups.

FLI-H: detector of P53 of Fluorescein isothiocyanate (FITC) fluorochrome.

Count: % of count cells labeled with anti Bcl-2

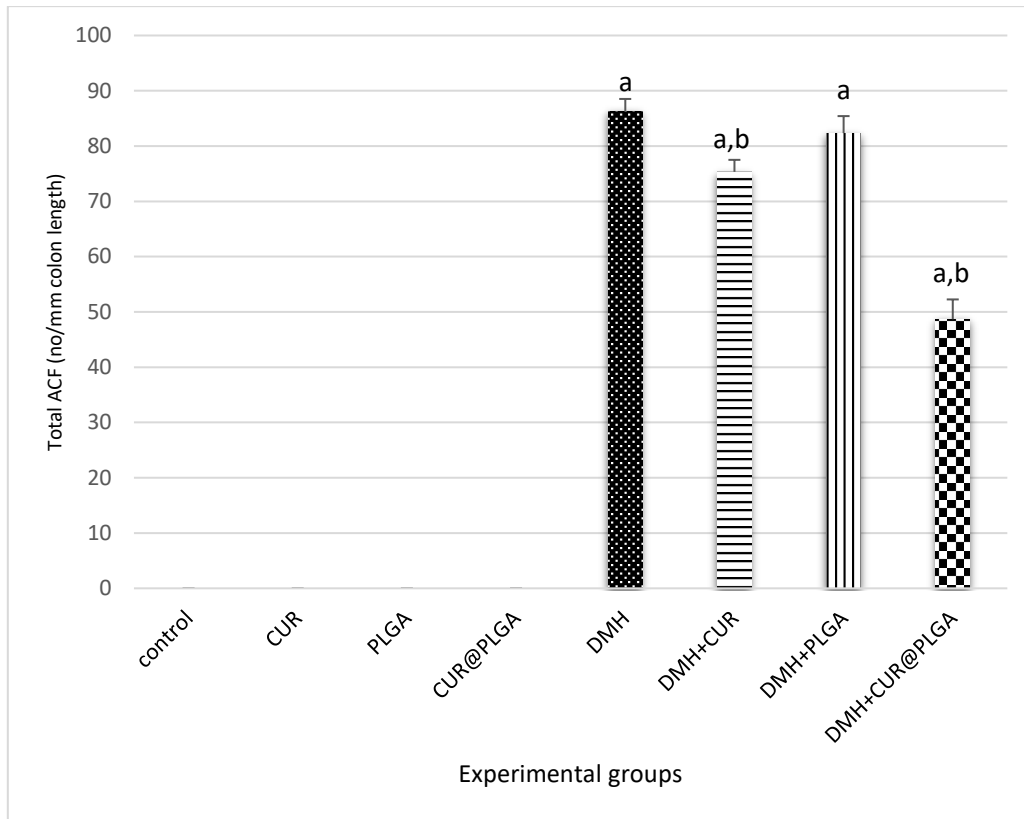


Fig. 4(a): Average total numbers of DMH-induced ACF in all groups under study; $P < 0.05$

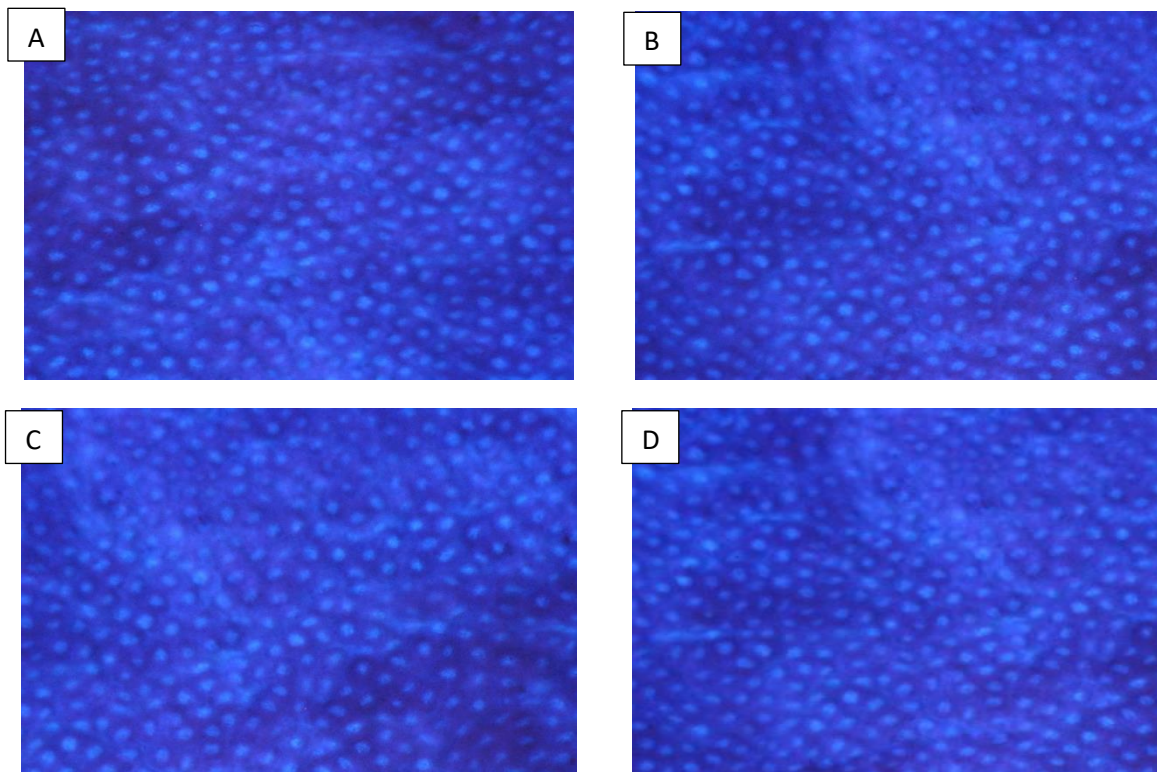


Fig.4 (b): Photomicrographs of normal mice whole colon stained with methylene blue (MB). A): Normal colonic mucosa; B): Colon of normal animal treated with curcumin (10 mg/kg body weight) showing normal colonic mucosa, MB, X200, bar= 50 μ m. C): Colon of normal animal treated with PLAGA (10 mg/kg body weight) showing normal colonic mucosa, MB, X200, bar= 50 μ m. D): Colon of normal animal treated with curcumin-encapsulated PLAGA (10 mg/kg body weight) showing normal colonic mucosa, MB, X200, bar= 50 μ m.

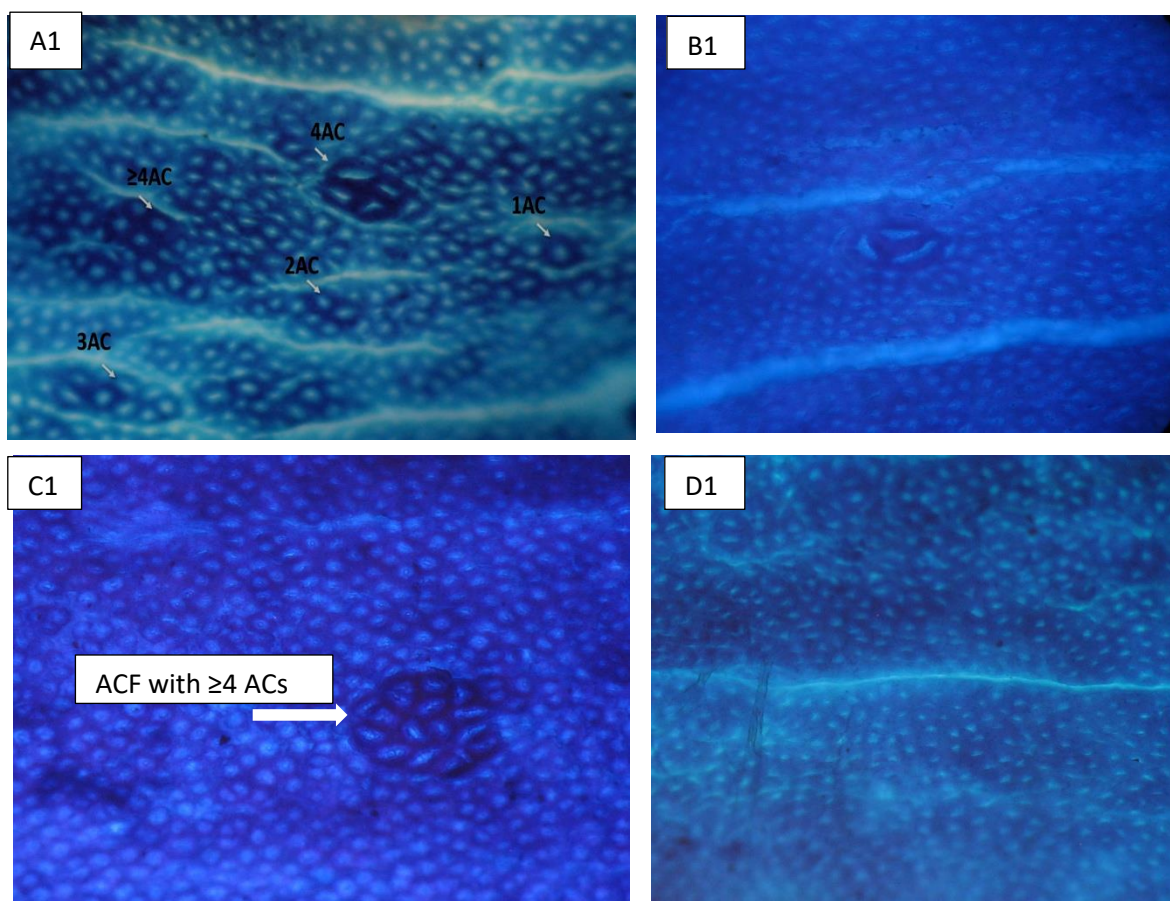


Fig.4 (c): Photomicrographs of treated mice whole colon stained with methylene blue (MB). A1): Colon of control positive animal treated with DMH (10 mg/kg body weight), showing increase total ACF and aberrant crypt with all numbers of ACs, MB, X200, bar= 50 μ m.; B1): Colon of diseased animal revived Curcumin (10 mg/kg body weight) showing aberrant crypt with 3 ACs and decrease aberrant crypt with ≥ 4 ACs also decrease total ACF, MB, X200, bar= 50 μ m. ; C1): Colon of diseased animal revived PLGA (10 mg/kg body weight) showing aberrant crypt with ≥ 4 ACs and increase in total ACF MB, X200, bar= 50 μ m. D1): Colon of diseased animal received curcumin-encapsulated PLGA (10 mg/kg body weight) showing mucosa with the most decreased number of ACF , MB, X200, bar= 50 μ m.

DISCUSSION

Using of plant based nontoxic materials including many dietary substances, to protect ,prevent, stop, or reverse the development of cancers is called chemoprevention, also many of those antioxidant substances naturally present in fruits and vegetables like lycopene, soy isoflavones, pomegranate phenolics, selenium and curcumin [26].

In [27] studies proved the stability of nanoparticle of curcumin that increased at least by 9 fold compared to that of plain curcumin by improving peroral bioavailability of curcumin. [28] prepared an optimized poly lactic-co-glycolic acid (PLGA) nano-formulation of curcumin that have 22-fold higher oral bioavailability in rats as compared to normal curcumin.

Colorectal cancer (CRC) is the third most common cancer in men and the second most common cancer in women worldwide and leading cause for cancer-related deaths so the trying to prevent it is a great goal throughout the world. The use of natural and nano-products provides efficient and safe chemopreventive agents to inhibit the progression of CRC [29].

The present study tends to evaluate the colon carcinogenicity effect of 1,2-dimethylhydrazine (DMH) and to explain the role of curcumin (CUR) and CUR encapsulated PLGA (CUR@PLGA) in alleviating the effect of DMH when administered to male mice.

In the present study the using of DMH cause elevation on MDA levels an end product of LPO and this in the line with the results of [30] that showed increasing levels of MDA during carcinogenesis were seen which may be due to DMH, that is considered as a methylating agent that may stimulates cell division and make colon tumor by elevated the level of ROS, which react with DNA.

In this study tissue MDA level significantly decreased in the DMH+CUR and DMH+CUR@PLGA groups when compared with DMH group and this agreed with the results of [31] that showed curcumin reduced oxidative stress and lipid peroxidation and attenuates aortic fatty streak development in rabbits that treated with atherogenicity diets. Also the present results in the same line with the results of [32] scientific report, 10 weeks of curcumin nanomicelle supplementation resulted in a statistically significant improvement in plasma levels of TAC, MDA, CRP and TNF- α in comparison to the placebo in asthenoteratospermia patients.

In fact ROS can also directly react with amino acid residues and made oxidative cleavage of the protein backbone producing protein carbonyl (PC). Also oxidation of lipids form reactive aldehydes which react with cysteine (Cys), histidine (His), arginine (Arg) and lysine (Lys) residues and thus form carbonyl groups. PC is an irreversible form of modification in protein and is a stable product. the determination of protein bound carbonyls is the most commonly used marker to assess protein oxidation [33].

The results of the present study showed elevation on PC levels in DMH group and compatible to these results [34] reported that PC contents in DMH-treated group was significantly higher than in nano CUR and all other groups ($p \leq 0.5$).

In this study the DMH+CUR and DMH+CUR@PLGA group showed significant decrease the PC levels when compared with DMH group and nano curcumin is better than normal CUR. These are in the line with [35] when study the improvement of cognitive function in aged female rats and accompanied by a decrease of lipid peroxidation in brain tissue when rats were treated with CUR. The properties of CUR as a free radical scavenging maybe due to its H-donating phenolic groups in its molecular structure [36].

In the present study, DMH administration caused a significant elevation of the reactive radical NO level and these results are in the line with [37] results that explained the action of DMH on enhancing the activity of nitric oxide synthetase (NOS). Excessive NO production by iNOS mRNA can produce damage to DNA.

The results of the present study showed decreased in DMH+CUR and DMH+CUR@PLGA groups on NO levels and also the greatest improvement was noticed on the nano group these findings are in line with those of the previous studies on the nanoCUR in various cancers of [38] who reported that there was a significant difference between cells treated with nanoCUR and cells treated with free CUR in the levels of NO and this action may be due to nanoCUR penetration through cell membrane inside cells is better than normal CUR. This explains that nanoCUR has a stronger antioxidant properties and protective effects against NO synthase, suggested as targets for CUR.

The level of all anti-oxidants on this study showed significant decrease on the DMH group when compared with normal group the same results expressed by the study of [39] and explained that by there are power ful antioxidant defense mechanisms against the toxic effects of active oxygen species in the body. Among them, superoxide dismutase (SOD) and catalase (CAT) are the important enzymes. Treatment with carcinogens or tumor promoters usually decreases levels of SOD and CAT, a decline in these enzymes may facilitate the initiation of oxidative processes, which would lead to the elevation of reactive oxygen species and consequently may account for increases in levels of oxidized DNA bases, credited for mutagenesis and carcinogenesis.

The present study agree with the [40] results of treatment with DMH decreased substantially the age related increase in GST activity. The treatment of animals with DMH induced decline in GST activity in liver and colorectal tissue may be due to their utilization in detoxification of carcinogenic metabolites of DMH.

The present study also in the line with the results of [41] who study the toxic effects of DMH on rats and find that decrease in colon GSH following DMH treatment. GSH depletion compounds the toxic insult from free radicals that result from anal ready impaired antioxidant detoxification system.

In this study DMH+CUR and DMH+CUR@PLGA groups showed significant increase in all antioxidants levels, this is also confirmed by [42] that study the effects of nano-CUR and CUR on the oxidant and antioxidant system in the liver mitochondria. Also the present results agreed with [43] that reported CUR can modulate the activity of SOD, CAT, GST, GSH and TAC levels cause of its great antioxidant properties.

According to the literature, the beneficial effects of CUR are associated with its structure. CUR has been reported to have two phenolic rings, which result in its potent antioxidant activity. In addition, CUR is a unique compound owing to its remarkable antioxidant, phenolic, and beta-ketone segments in its structure [42]. However, studies have denoted that the protective effects of CUR are less significant compared to its nano capsule forms since CUR has considerably low solubility and bioavailability [44]. On the other hand, more recent findings have shown that nano-CUR could be used to compensate for some of the limitations of curcumin (e.g., low solubility and bioavailability) [45]. The results of the present study also confirmed the efficiency and better outcomes of CUR nanoparticles compared to CUR alone.

In this study we investigated the expression of p53, Caspase3, Bcl-2 and Bax using flowcytometric technique to understand the signaling mechanism related to the anti-apoptotic efficacy of nanoCUR against colorectal carcinogenesis.

In the introduced study using of DMH cause reduce on the levels of p53, Caspase3, Bax and elevation on Bcl-2, this the same results of [46] and it was explained as a apoptosis has an essential role in maintaining normal colonic epithelia. The normal structure of colonic crypts is maintain by a dynamic equilibrium between apoptosis at the top of the crypt and cell proliferation at the base. There is growing evidence displaying the presence of unbalance of cell growth and apoptosis rates during CRC formation by using DMH.

Therefore, in the current study, it was found that there was a significant increase in the levels of P53, Bax and Caspase-3 accompanied by a significant reduce in the expression level of Bcl-2 in DMH+CUR and DMH+CUR@PLGA groups when compared to DMH group. Thus, these results are the same for [47] indicated that p53 induces apoptosis in nanoCUR group through the activation of a Caspase cascade pathway. The results of the present study also confirmed the efficiency and better outcomes of CUR nanoparticles compared to CUR alone.

The effect of CUR and nanoCUR on caspase-3 in the current study is the same with [48] and this may be due to the necessary of caspase-3 for the fragmentation of DNA and the morphological changes associated with apoptosis.

The proteins of the Bcl-2 family are regulators of apoptosis, their functions include pro-apoptotic (Bax, Bak and Bad) or anti-apoptotic (Bcl-2 and Bcl-XL) regulators. Also, p53 induces expression of Bax that is the main intrinsic pathway of apoptosis. In the other hand the up regulation of Bax cause the stimulation of cytochrome C released from mitochondria that lead to Caspase activation to perform apoptosis with inhibition expression of the Bcl-2 [49].

The Bcl-2 protein is normally expressed along the crypts of normal colonic epithelium relative to the stem cell division where the apoptosis rate is low also Bcl-2 is linked to the early stage of CRC development [50]. CUR was found to increase Bax expression and decrease Bcl-2 in colon adenocarcinoma through the activation of p53 [51].

The suggested multistep of colon carcinogenesis may start when aberrant crypt foci (ACF) appear in the colon. ACF were determined as lesions composed of enlarged crypts, slightly elevated above the surrounding mucosa and more densely stained with methylene blue than normal crypts [52].

Using of DMH cause DNA methylation resulting in ACF formation in mice colons [53-55]. These studies are in line with the present study as the DMH group showed significant increase in the number of ACF. However using CUR and nanoCUR showed great significant decreased of ACF the same with [56] and [57] this may be due

to the effect of CUR on DNA methylation by inhibition of DNA methyl-transferase enzyme. Even in the present study normal CUR group has significant reduced numbers of ACF but CUR encapsulated PLGA reduced it more strongly than CUR alone and this is in the line with [58].

CONCLUSION

CUR-loaded PLGA nanoparticles improved cellular uptake, which induced apoptosis and suppressed tumor cell proliferation. Also it improved bioavailability and prolonged half-life instead of the free CUR.

ACKNOWLEDGEMENT

The authors would like to make acknowledgements to professor El-Sayed M Elhabibi who assist me to complete my thesis successfully before he unfortunately passed away.

REFERENCES

- [1] Ferlay, J., et al., *Estimating the global cancer incidence and mortality in 2018: GLOBOCAN sources and methods*. International Journal of Cancer, 2019. **144**(8): p. 1941-1953.
- [2] Venkatachalam, K., et al., *Biochemical and molecular aspects of 1, 2-dimethylhydrazine (DMH)-induced colon carcinogenesis: a review*. Toxicology Research, 2020.
- [3] Fang, J., J. Lu, and A. Holmgren, *Thioredoxin reductase is irreversibly modified by curcumin a novel molecular mechanism for its anticancer activity*. Journal of biological chemistry, 2005. **280**(26): p. 25284-25290.
- [4] McLellan, E.A. and R.P. Bird, *Aberrant crypts: potential preneoplastic lesions in the murine colon*. Cancer research, 1988. **48**(21): p. 6187-6192.
- [5] Danhier, F., et al., *PLGA-based nanoparticles: an overview of biomedical applications*. Journal of controlled release, 2012. **161**(2): p. 505-522.
- [6] Yallapu, M.M., et al., *Fabrication of curcumin encapsulated PLGA nanoparticles for improved therapeutic effects in metastatic cancer cells*. Journal of colloid and interface science, 2010. **351**(1): p. 19-29.
- [7] Sankar, P., et al., *Immunomodulatory effects of nanocurcumin in arsenic-exposed rats*. International immunopharmacology, 2013. **17**(1): p. 65-70.
- [8] Ismail, E., et al., *Synthesis and Characterization of some Ternary Metal Complexes of Curcumin with 1, 10-phenanthroline and their Anticancer Applications*. Journal of Scientific Research, 2014. **6**(3): p. 509-519.
- [9] Gunasekaran, S., et al., *Structural Investigation on Curcumin*. Asian Journal of Chemistry, 2008. **20**(4): p. 2903.
- [10] Lu, H., et al., *Prevention of development of N, N'-dimethylhydrazine-induced colon tumors by a water-soluble extract from cultured medium of Ganoderma lucidum (Rei-shi) mycelia in male ICR mice*. International journal of molecular medicine, 2002. **9**(2): p. 113-117.
- [11] Satapathy, A., M.V.J.R.J.o.P. Rao, and Technology, *Protective effect of Curcumin on 2, 4-Dichlorophenoxy acetic acid exerted Hepatotoxicity in Mice*. 2018. **11**(2): p. 637-642.
- [12] Oyeyemi, O., et al., *Curcumin-artesunate based polymeric nanoparticle; antiplasmodial and toxicological evaluation in murine model*. Frontiers in pharmacology, 2018. **9**: p. 562.
- [13] Bird, R.P., *Role of aberrant crypt foci in understanding the pathogenesis of colon cancer*. Cancer letters, 1995. **93**(1): p. 55-71.
- [14] Bird, R.P., *Observation and quantification of aberrant crypts in the murine colon treated with a colon carcinogen: Preliminary findings*. Cancer Letters Cancer Letters, 1987. **37**(2): p. 147-151.
- [15] Tribukait, B., G. Moberger, and A. Zetterberg, *Methodological aspects of rapid-flow cytofluorometry for DNA analysis of human urinary bladder cells*. Pulse Cytophotometry, 1975. **1**: p. 50.
- [16] Ohkawa, H., N. Ohishi, and K. Yagi, *Assay for lipid peroxides in animal tissues by thiobarbituric acid reaction*. Analytical biochemistry, 1979. **95**(2): p. 351-358.
- [17] Montgomery, H. and J. Dymock, *Nitrite assay in tissue fluids*. Analyst, 1961. **86**: p. 414.
- [18] Levine, R.L., et al., *[49] Determination of carbonyl content in oxidatively modified proteins*, in *Methods in enzymology*. 1990, Elsevier. p. 464-478.

- [19] Koracevic, D., et al., *Method for the measurement of antioxidant activity in human fluids*. Journal of clinical pathology, 2001. **54**(5): p. 356-361.
- [20] Aebi, H., [13] *Catalase in vitro*, in *Methods in enzymology*. 1984, Elsevier. p. 121-126.
- [21] Nishikimi, M., N.A. Rao, and K. Yagi, *The occurrence of superoxide anion in the reaction of reduced phenazine methosulfate and molecular oxygen*. Biochemical and biophysical research communications, 1972. **46**(2): p. 849-854.
- [22] Beutler, E., *Improved method for the determination of blood glutathione*. J. lab. clin. Med., 1963. **61**: p. 882-888.
- [23] Habig, W.H., M.J. Pabst, and W.B. Jakoby, *Glutathione S-transferases the first enzymatic step in mercapturic acid formation*. Journal of biological Chemistry, 1974. **249**(22): p. 7130-7139.
- [24] Dean, P.N. and J.H.J.T.J.o.c.b. Jett, *Mathematical analysis of DNA distributions derived from flow microfluorometry*. 1974. **60**(2): p. 523.
- [25] Snedecor, G. and W.J.T.I.s.u.p. Cochran, Ames, Iowa, USA, *Statistical method 7th Ed*. 1980: p. 39-63.
- [26] Hamiza, O.O., et al., *Amelioration of 1, 2 Dimethylhydrazine (DMH) induced colon oxidative stress, inflammation and tumor promotion response by tannic acid in Wistar rats*. Asian Pac J Cancer Prev, 2012. **13**(9): p. 4393-4402.
- [27] Shaikh, J., et al., *Nanoparticle encapsulation improves oral bioavailability of curcumin by at least 9-fold when compared to curcumin administered with piperine as absorption enhancer*. European Journal of Pharmaceutical Sciences, 2009. **37**(3-4): p. 223-230.
- [28] Tsai, Y.-M., et al., *Optimised nano-formulation on the bioavailability of hydrophobic polyphenol, curcumin, in freely-moving rats*. Food chemistry, 2011. **127**(3): p. 918-925.
- [29] Sharma, S.H., et al., *Molecular chemoprevention by morin—a plant flavonoid that targets nuclear factor kappa B in experimental colon cancer*. Biomedicine & Pharmacotherapy, 2018. **100**: p. 367-373.
- [30] Aziza, S., S. Abdel-Aal, and H. Mady, *Chemopreventive effect of curcumin on oxidative stress, antioxidant status, DNA fragmentation and caspase-9 gene expression in 1, 2-dimethylhydrazine-induced colon cancer in rats*. American J Biochem Mol Biol, 2014. **4**: p. 22-34.
- [31] Quiles, J.L., et al., *Curcuma longa extract supplementation reduces oxidative stress and attenuates aortic fatty streak development in rabbits*. 2002. **22**(7): p. 1225-1231.
- [32] Alizadeh, F., et al., *Curcumin nanomicelle improves semen parameters, oxidative stress, inflammatory biomarkers, and reproductive hormones in infertile men: A randomized clinical trial*. 2018. **32**(3): p. 514-521.
- [33] Weber, D., M.J. Davies, and T. Grune, *Determination of protein carbonyls in plasma, cell extracts, tissue homogenates, isolated proteins: focus on sample preparation and derivatization conditions*. Redox biology, 2015. **5**: p. 367-380.
- [34] Eboh, A., L. Chuku, and A. Uwakwe, *Chemopreventive influence of kolaviron on 1, 2-dimethylhydrazine induced plasma carbonyl content and non-enzymatic antioxidant status in rat colon carcinogenesis*. Sch. Acad J. Pharm, 2015. **4**(2): p. 81-87.
- [35] Akomolafe, S.F., et al., *Curcumin Administration Mitigates Cyclophosphamide-Induced Oxidative Damage and Restores Alteration of Enzymes Associated with Cognitive Function in Rats' Brain*. 2020. **38**(1): p. 199-210.
- [36] Barclay, L.R.C., et al., *On the antioxidant mechanism of curcumin: classical methods are needed to determine antioxidant mechanism and activity*. Organic letters, 2000. **2**(18): p. 2841-2843.
- [37] Samanta, S., et al., *Protective effects of vanadium against DMH-induced genotoxicity and carcinogenesis in rat colon: removal of O6-methylguanine DNA adducts, p53 expression, inducible nitric oxide synthase downregulation and apoptotic induction*. Mutation Research/Genetic Toxicology and Environmental Mutagenesis, 2008. **650**(2): p. 123-131.
- [38] Rami, A. and N. Zarghami, *Comparison of inhibitory effect of curcumin nanoparticles and free curcumin in human telomerase reverse transcriptase gene expression in breast cancer*. Advanced Pharmaceutical Bulletin, 2013. **3**(1): p. 127.
- [39] Rajeshkumar, N. and R.J.C.I. Kuttan, *Modulation of carcinogenic response and antioxidant enzymes of rats administered with 1, 2-dimethylhydrazine by Picroliv*. 2003. **191**(2): p. 137-143.
- [40] Mohania, D., et al., *Anticarcinogenic effect of probiotic Dahi and piroxicam on DMH-induced colorectal carcinogenesis in Wistar rats*. 2013. **1**(1): p. 8-24.
- [41] Pence, B.C.J.T.J.o.n., *Dietary selenium and antioxidant status: toxic effects of 1, 2-dimethylhydrazine in rats*. 1991. **121**(1): p. 138-144.
- [42] Ranjbar, A., et al., *EEffects of nano-curcumin and curcumin on the oxidant and antioxidant system of the liver mitochondria in aluminum phosphide-induced experimental toxicity*. 2020. **7**(1): p. 58-64.

- [43] Al-Rubaei, Z., T.U. Mohammad, and L.K. Ali, *Effects of local curcumin on oxidative stress and total antioxidant capacity in vivo study*. Pak J Biol Sci, 2014. **17**(12): p. 1237-1241.
- [44] Głombik, K., et al., *Curcumin influences semen quality parameters and reverses the di (2-ethylhexyl) phthalate (DEHP)-induced testicular damage in mice*. 2014. **66**(5): p. 782-787.
- [45] Rahimi, H.R., et al., *Novel delivery system for natural products: Nano-curcumin formulations*. 2016. **6**(4): p. 383.
- [46] Watson, A.J. and D.M. Pritchard, *VII. Apoptosis in intestinal epithelium: lessons from transgenic and knockout mice*. American Journal of Physiology-Gastrointestinal and Liver Physiology, 2000. **278**(1): p. G1-G5.
- [47] Panda, A.K., et al., *New insights into therapeutic activity and anticancer properties of curcumin*. Journal of experimental pharmacology, 2017. **9**: p. 31.
- [48] Hanna, D.H. and G.R. Saad, *Nanocurcumin: preparation, characterization and cytotoxic effects towards human laryngeal cancer cells*. RSC Advances, 2020. **10**(35): p. 20724-20737.
- [49] Anto, R.J., et al., *Curcumin (diferuloylmethane) induces apoptosis through activation of caspase-8, BID cleavage and cytochrome c release: its suppression by ectopic expression of Bcl-2 and Bcl-xl*. Carcinogenesis, 2002. **23**(1): p. 143-150.
- [50] Van Der Heijden, M., et al., *Bcl-2 is a critical mediator of intestinal transformation*. Nature communications, 2016. **7**(1): p. 1-11.
- [51] Song, G., et al., *Curcumin induces human HT-29 colon adenocarcinoma cell apoptosis by activating p53 and regulating apoptosis-related protein expression*. Brazilian journal of medical and biological research, 2005. **38**(12): p. 1791-1798.
- [52] Fuku, N., et al., *Effect of running training on DMH-induced aberrant crypt foci in rat colon*. Medicine & Science in Sports & Exercise, 2007. **39**(1): p. 70-74.
- [53] Jackson, P.E., et al., *The relationship between 1, 2-dimethylhydrazine dose and the induction of colon tumours: tumour development in female SWR mice does not require a K-ras mutational event*. Carcinogenesis, 1999. **20**(3): p. 509-513.
- [54] Essawy, S.S., et al., *Effect of celecoxib and cisplatin combination on apoptosis and cell proliferation in a mouse model of chemically-induced colonic aberrant crypt foci*. Egyptian journal of basic and applied sciences, 2017. **4**(4): p. 323-331.
- [55] Luo, L. and T.P. Pretlow, *DNA methylation in human aberrant crypt foci (ACF), putative precursors of colorectal cancer*. 2004, AACR.
- [56] Patel, V.B., et al., *Colorectal cancer: chemopreventive role of curcumin and resveratrol*. Nutrition and cancer, 2010. **62**(7): p. 958-967.
- [57] Hassan, F.-u., et al., *Curcumin as an alternative epigenetic modulator: Mechanism of action and potential effects*. Frontiers in genetics, 2019. **10**: p. 514.
- [58] Chaudhary, A., et al., *Chemoprevention of colon cancer in a rat carcinogenesis model using a novel nanotechnology-based combined treatment system*. 2011. **4**(10): p. 1655-1664.